

# STATE-SPACE BIOLOGICAL NEURON MODEL DYNAMICS IN MULTIPLE SCLEROSIS

Erica Liu (20944002)

Aidan Kirwin (20957489)

Connor Irvine (20947051)

Salma Abdelfattah (20956717)

Keenan Ung (20947443)

**Abstract** – The primary effect of the inflammatory response associated with Multiple Sclerosis (MS) is damage to the myelin in the central nervous system (CNS) [1]. Myelin enables saltatory conduction along the axon. As a result, demyelination affects both conduction velocity and, consequently, neural activity in the CNS [1]. To investigate the effects of demyelination, three simulations were conducted on a state-space biological neuron model. The model consists of a Hodgkin-Huxley circuit analog model representing unmyelinated axon segments, and a single cable model representing myelinated segments (internodes). The simulations examined three different effects: the gradual deterioration of myelin at every myelinated region along an axon, the complete loss of myelin for an increasing number of internodes, and the substitution of myelinated regions with Nodes of Ranvier. The first simulation indicated a negative correlation between conduction velocity, firing rate, and myelin degradation. The second simulation showed a similar relationship between an increasing number of completely demyelinated regions and conduction velocity and firing rate. The third simulation found a greater firing rate and conduction velocity for axons with many internodes versus those with fewer internodes. This report aims to apply the observed relationships to quantify how demyelination translates to physiological symptoms.

**Keywords** – *neuron modelling, demyelination, Hodgkin-Huxley, single-cable model, multiple sclerosis.*

## I. INTRODUCTION

Multiple Sclerosis (MS) is an autoimmune disease affecting the central nervous system (CNS) [1]. A recent epidemiological report on MS reported that around 2.8 million people have been diagnosed with MS worldwide, with the onset of symptoms typically occurring between the ages of 20-40 years [2,3]. The immune response involved in MS causes damage to myelin-forming glial cells, disrupting the normal flow of electrical impulses along the nerves [1]. Among the numerous symptoms associated with MS, various studies have reported reduced neuronal firing rates with an increased weakness in voluntary muscle activation [4].

While there are currently no cures for MS, there are numerous treatment options that contribute to managing and slowing the progression of MS symptoms, some of which include drug therapies, including disease-modifying and anti-inflammatory therapies, in addition to physical therapies, deep-brain stimulation, and cognitive rehabilitation [5, 6]. Given that there are no current cures for this disease, it is essential for researchers to continue studying the disease to further understand its mechanisms and be able to develop more effective treatment plans by understanding the progression of the disease. Having personalized treatment plans can optimize patient outcomes and their overall quality of life.

To further enable this learning and investigate the progression of MS, this study aimed to develop a computational model that investigates the effects of demyelination, caused by MS, on neuronal firing rate and conduction velocity. To achieve these objectives, neuron models currently used in literature were explored. The Hodgkin-Huxley model was utilized to simulate the propagation of an action potential in a Node of Ranvier by representing the axonal membrane in terms of circuit components [7]. A circuit analog single-cable model found in literature was used to model the myelinated sections of the axons (internodes) [8, 9].

Using a combination of the aforementioned models, neurons were simulated under three conditions: (a) varying myelination of internodes; (b) simulating the removal of internodes by

drastically decreasing the number of myelin wraps for each internode, in succession; (c) increasing the ratio of Nodes of Ranvier (nodes) to internodes.

Each simulation will provide measures of conduction velocity and firing rate (neuronal activity) at different parameter settings. These results will be discussed in the context of MS: effects of demyelination on neural activity, and progression of symptoms. The relationship between the thinning/damaging of myelin sheath with firing rate, and the impact this could have on physiological processes will be examined.

## II. EXPERIMENTAL METHODS

### A. Conceptual Overview of Model

Nodes of Ranvier are unmyelinated sections of the axon. The Hodgkin-Huxley (H-H) circuit analog module was used to represent these segments [7]. The output of one H-H segment is a voltage  $V_m$ , representing the membrane potential across the axon membrane. The circuit schematic of the H-H model can be seen in Fig. A.1.

Internodes represent myelinated regions of the axon. A single cable circuit analog model was used to represent these segments, using a parallel resistor-capacitor (RC) circuit to represent the myelin sheath and approximate the behaviour of internodes [8,9]. A double cable model is also discussed in [9]. The double-cable model provides an analog for the resistance and capacitance of both the axon and myelin sheath, whereas the single-cable model does not, and can thus be used to model the potential difference between the extracellular space and the periaxonal space [9]. The double-cable model was found to be highly unstable for small changes in its parameters, including experimental factors (myelin thickness). The single-cable model is lower resolution, but the objectives of this study do not require analysis of the periaxonal space. The single cable model was therefore used due to its robustness. The circuit schematic of the single-cable internode model is given in Fig. A.2.

The neuron model therefore combines a set of H-H nodes and single-cable internodes in sequence to represent the length of a single axon. Each segment's buffered output serves as the input to the subsequent segment. In theory, the voltage of each segment at different points in time should reflect the behavior of an action potential traversing an axon. By chaining segments in a sequence, the axon representation as visualized in Fig. A.3 was achieved.

### B. State Variables and Equations

Two sets of equations were used in the model: one for the H-H segments and one for the internode segments. The H-H node equations are shown in Appendix C.4.1. The equations were taken from [7]. Note that the H-H model is not provided in state-space form, as the model consists of non-linear differential equations. All state variables are defined in Appendix C.4.1.

The internode state equation is shown in Appendix C.4.2. It is derived from the circuit shown in Fig. A.2. The derivation of the state equation can be seen in Appendix B. All state variables are defined in Appendix C.4.2.

### C. Functions: Conduction Velocity and Firing Rate

Three simulations were conducted to evaluate the effects of demyelination. Each simulation varies a set of parameters that address the different ways demyelination affects the conduction velocity and maximum firing rate of an axon. Conduction velocity is defined as the distance along an axon an action potential impulse travels per unit time. The MATLAB function used to calculate conduction

velocity is provided in Appendix D. The firing rate is measured as the number of action potential spikes per unit time. The function used to evaluate the firing rate is provided in Appendix D.

#### D. *Simulation 1: Varying Myelin Thickness*

Simulation 1 examines the effect of gradually deteriorating myelin for all internodes along the axon. Axons were simulated with a starting myelin thickness of 202.5 nm (corresponding to 27 myelin wraps,  $n$ , as defined in Appendix C.2.), and simulations were run for axons of decrementally thinner myelin sheaths in intervals of 7.5 nm. While axon radius in a human tends to vary between 0.6-10  $\mu\text{m}$  [10], yielding an axon thickness range of approximately 180 - 6000 nm per Equation (C.3), it was observationally determined that the response variables of interest (conduction velocity and firing rate) plateaus prior to 200 nm. A pulse function, representing a current injection with a pulse-width of 74 ms and an amplitude of -30  $\mu\text{A}$ , was used as an input for all three simulations. The implementation of Simulation 1 can be found in Appendix E.1.

#### E. *Simulation 2: Demyelination at Internodes*

Simulation 2 examines the effect of demyelinated internodes. Rather than changing the degree of myelination for all nodes (as is done in Simulation 1), internodes were instead ‘demyelinated’ one at a time. The single-cable model does not technically allow for complete myelination, as this would mean the number of myelin wraps ( $n$ ) would be equal to 0, yielding infinite conductance and capacitance values per Equations (C.1)-(C.2). A value of  $n = 0.5$  myelin wraps was chosen to represent a demyelinated internode. An axon beginning with 10 internodes and 11 nodes was constructed, each internode possessing a 250 nm myelin sheath. The model was then simulated, and the conductance velocity and firing rate were recorded. Then, one of the 10 internodes would be demyelinated (i.e.  $n = 0.5$ ). The model was then simulated again, and the data was recorded. This continued until every internode was demyelinated. The implementation of Simulation 2 can be found in Appendix E.2.

#### F. *Simulation 3: Varying the Number of Nodes*

Simulation 3 investigated the role of internodes in the axon. It looked at the effects of replacing myelinated regions of internodes with H-H nodes. This was intended to elucidate the role of myelin in saltatory conduction by comparing an axon with a high abundance of myelinated regions with the same axon as its internodes are replaced with Nodes of Ranvier. The implementation of Simulation 3 can be found in Appendix E.3.

### III. EXPERIMENTAL RESULTS

The conduction velocity and firing rate were assessed for varying myelin thicknesses, as presented in Fig. 1.A. In Fig. 1.B, two conduction velocities were calculated: true and node velocity. Using metrics outlined in Preston and Barbara [11], it was reported an internode length is around 1mm, while the length of a node of Ranvier is between 1 to 2  $\mu\text{m}$ . While the node velocity is found as the quotient of the total axon length, including both nodes and internodes, and the total time taken for the signal to travel through the axon, the true velocity follows a similar calculation but accounts for the internodal length.

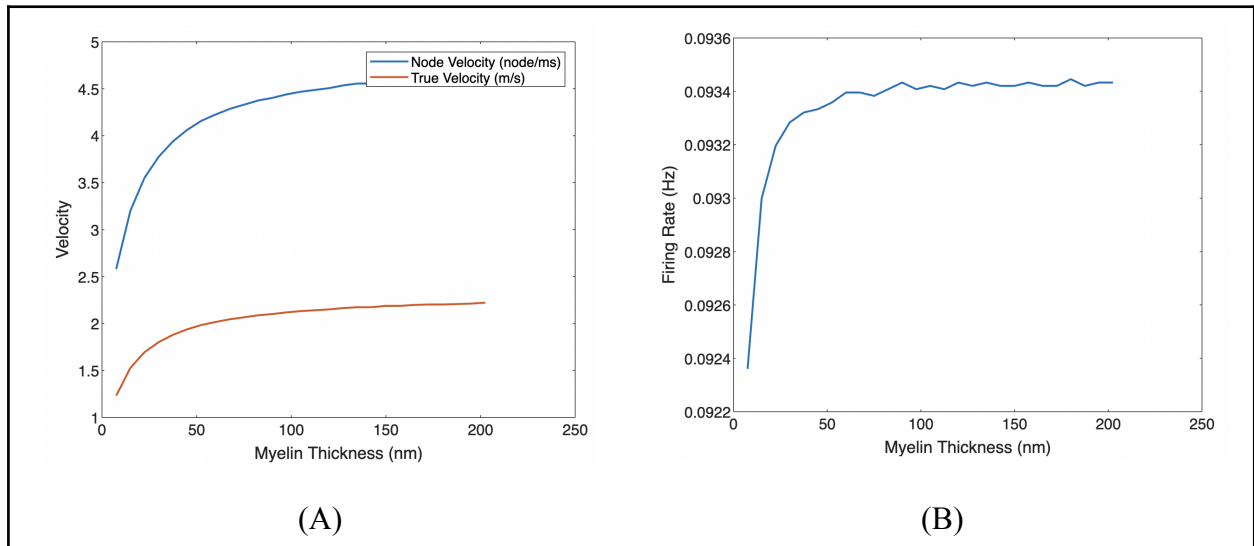


Fig. 1. Results of simulation 1; (A) conduction velocity (m/s) as a function of myelin thickness (nanometers); (B) firing rate (Hz) as a function of myelin thickness.

Due to the difficulty of accurately estimating the lengths of the nodes and internodes due to their variability, plotting the true and node (estimated) velocities can be used to determine how varying the node lengths can affect their associated conduction velocities.

Simulation 2, involving the ‘removal’ of myelin from the internodes, was analyzed similarly to the preceding simulation. In this case, the conduction velocity and firing rate were analyzed over the number of demyelinated nodes, as shown in Fig. 2. Exhibited in Fig. 2. A, the true and node velocities were calculated, similar to Simulation 1, to investigate the impact of the internode and node lengths on the conduction velocities.

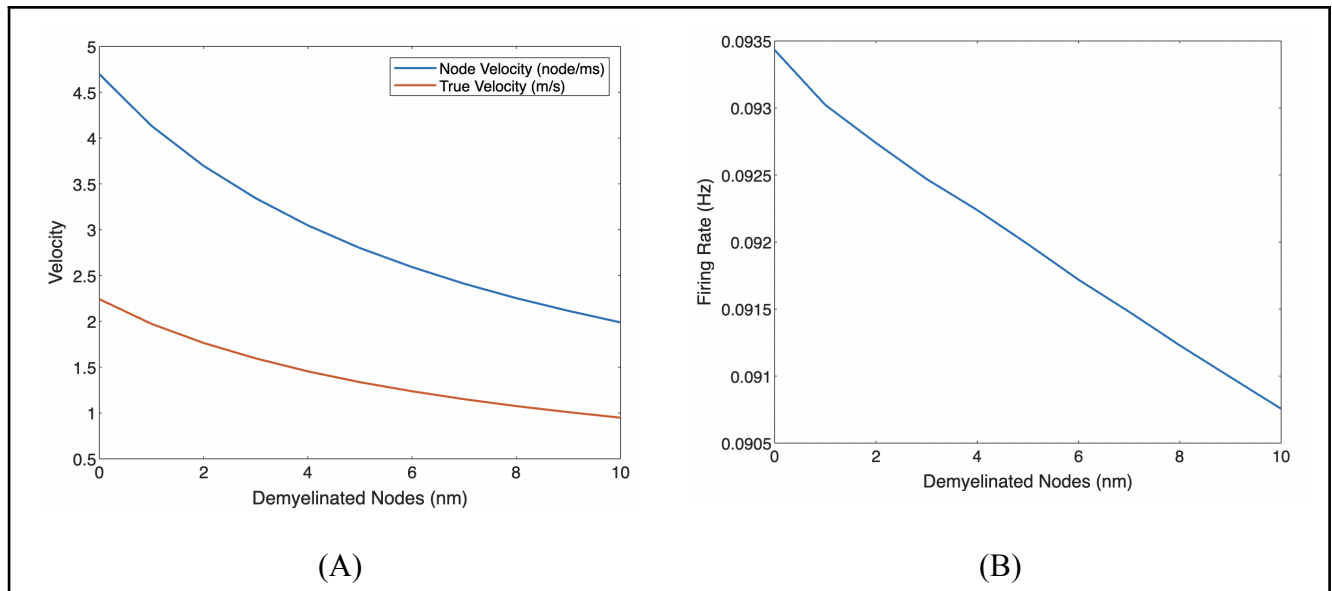


Fig. 2. Results of simulation 2; (A) conduction velocity (m/s) as a function of demyelinated nodes; (B) firing rate (Hz) as a function of demyelinated nodes.

The estimated slope of the node conduction velocity is approximately  $-0.2406$  m/s/demyelinated node, while the slope of the true conduction velocity was approximately  $-0.1149$  m/s/demyelinated node. Similarly, the calculated slope for the firing rate was found to be  $-0.0025$  Hz/demyelinated node.

Similar plots were also generated for visualizing the results of Simulation 3, as shown in Fig. 3. While still maintaining a constant axon length with 21 segments of nodes and internodes, the number of internodes were incrementally replaced by nodes. The associated conduction velocity and firing rate for each internode replacement were calculated and displayed in the figure below.

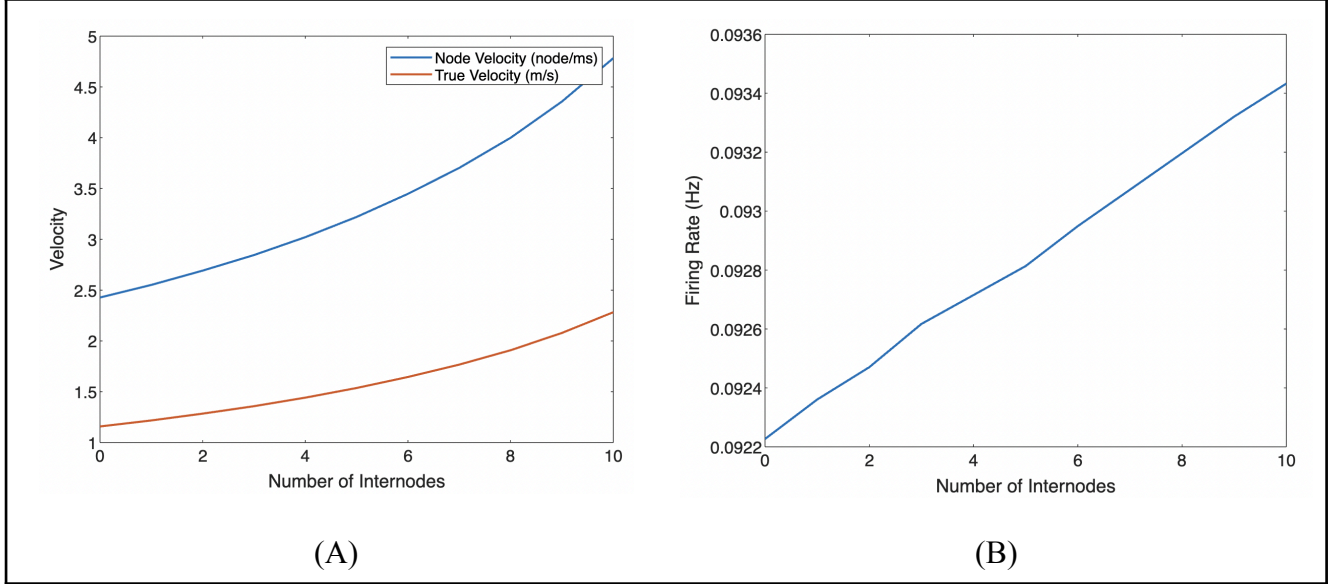


Fig. 3. Results of simulation 3; (A) conduction velocity (m/s) as a function of the number of internodes; (B) firing rate (Hz) as a function of the number of internodes.

#### IV. VERIFICATION AND VALIDATION

##### A. Verification Activities and Results

Unit tests were performed to verify various functions. Code reviews were also performed as a sanity check to confirm the correctness of equations. All verification activities are tabulated in Appendix F.

While all verification activities passed, it is important to note that the firing rate unit test revealed an issue with the firing rate calculation; when passed a sawtooth wave with a frequency of 50 Hz, the returned frequency was slightly higher. When graphing the wave with its peaks highlighted, it was noted that the firing rate function counted one too many peaks, causing it to return a higher frequency.

##### B. Validation Activities and Results

The simulation results were validated through comparison to existing literature regarding the action potentials of nodes and internodes. There are many existing models of action potentials at nodes, such as the one developed by S. Reutskiy et al. [12]. The model takes a pulse current input of length 0.01 ms and amplitude of 4 nA [12]. To validate our model, the input had to be adjusted to match the model from literature, however, as a current input of such a short duration and a small amplitude could not generate an action potential. Thus, an input pulse current of length 1ms and amplitude of 40  $\mu$ A was used. The offset of -70 was changed to 0 to better match the data for comparison purposes. The data of the model from literature was pulled using WebPlotDigitizer [13] and compared to our model, as can be seen in Fig. 4. The time also had to be normalized due to the low speed of our model.

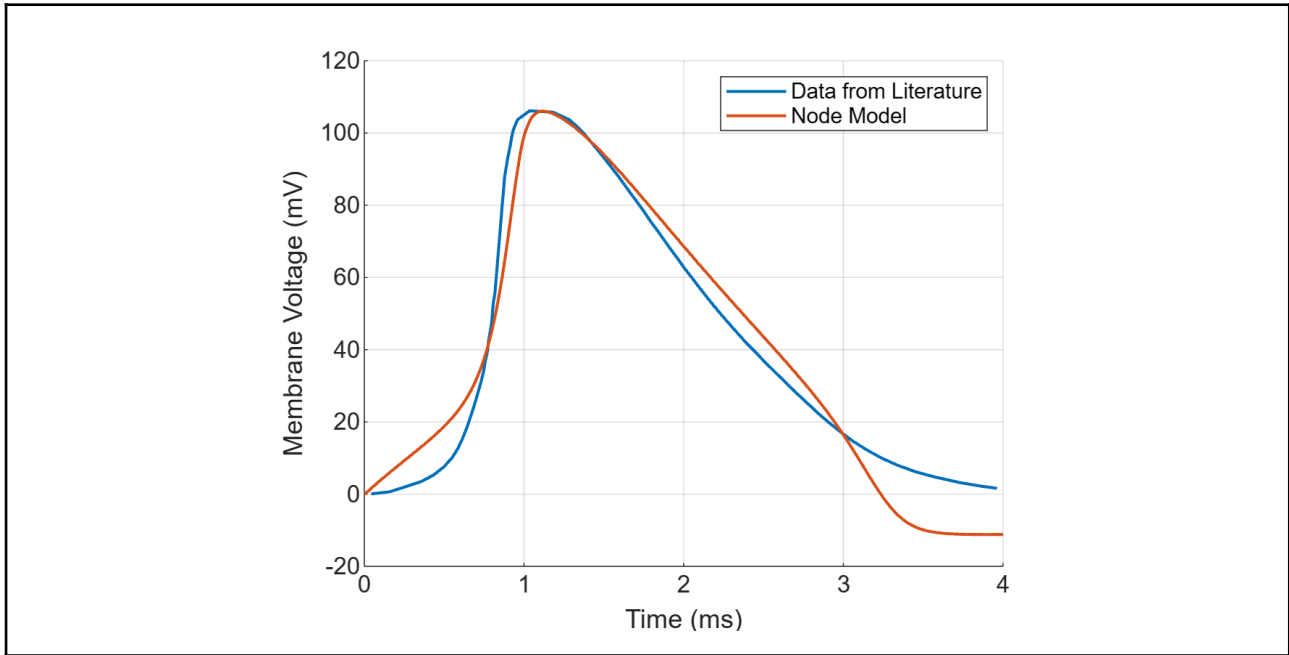


Fig. 4. Comparison test between the proposed H-H model and a similar circuit analog model from [12].

The model generally matches the data from literature, however, there is a distinct lack of the hyperpolarization phase, as the standard model for an action potential usually depicts. This absence of the hyperpolarization phase was generally consistent across literature, as many models neglect the hyperpolarization phase. It is not known why this phase is not included in many models.

Regarding the internode, few papers model the action potential at the internode. Our model also does not account for changes in the myelin thickness close to the edge at the paranode; due to the low resolution of our model, an internode waveform similar to the internode in Fig. 5.A would prevent the propagation of the action potential along the axon. As a result, the “internode” in our model can be seen as a combination of the paranode, juxtaparanode, and internode shown in Fig. 5.A from [14].

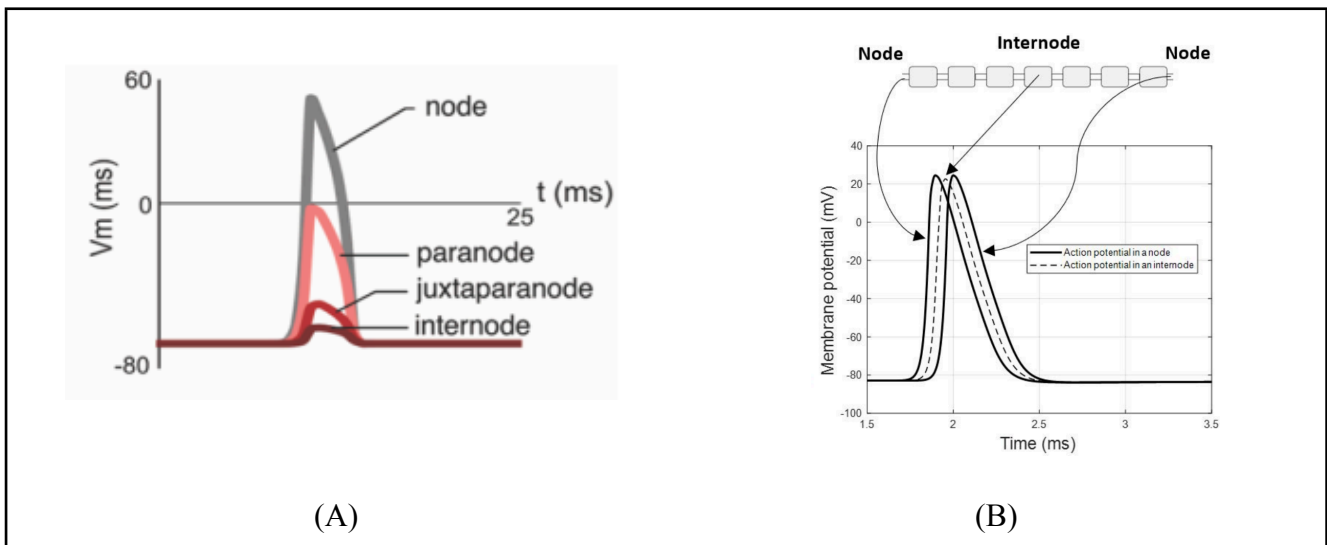


Fig. 5. (A) Internode model from [14]; (B) Internode model from [15]

Based on both Fig. 5.A and 5.B [15], one can extrapolate that the shape of the action potential at the node and internode are similar, with the internode delayed and having a lower amplitude. This aligns with our model, as can be shown in Fig. 6.

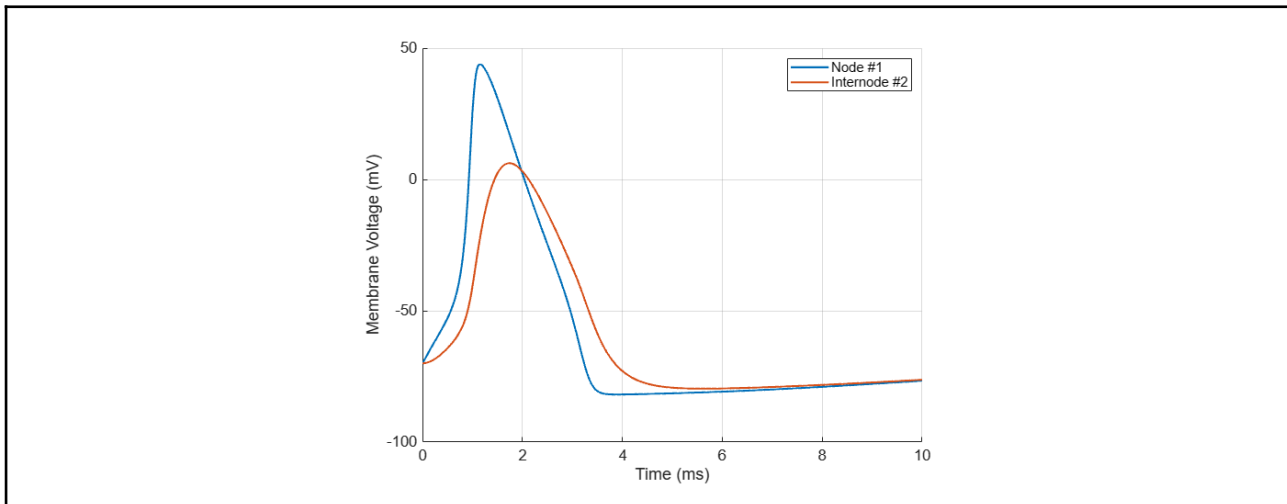


Fig. 6. The action potential waveform generated by our model for a node and internode in sequence.

Regarding Simulation 1 where the myelin thickness is varied, the results generally align with expected values from literature. Based on research, when 25% of the myelin sheath is removed, the change in conduction velocity is negligible, however, when 100% of the myelin is removed, the CV decreased by at least 38 +/- 10%, depending on how many segments were demyelinated [14].

According to research by [14], when the thickness of the myelin sheath approaches 0, a steep decrease in the CV is observed, as shown in Fig. 7. Our model cannot handle cases where the myelin sheath is entirely absent at the internodes, so we took a value of 0.5 myelin wraps to represent a demyelinated internode for Simulation 2 and a minimum myelin thickness of 7.5 nm in Simulation 1.

Simulation 1 studied the effect of the amount of myelin removed on the conduction velocity and our results showed a steep drop-off when the myelin thickness was reduced to under 50 nm. This trend aligns with a study conducted by S. Reutskiy et al., on the effect of demyelination on conduction speed [12]. The effect of demyelination is quantified through the change in thickness and normalizing the result. Fig. 7 shows the data from literature, which shows a similar relationship to Fig. 1.A.



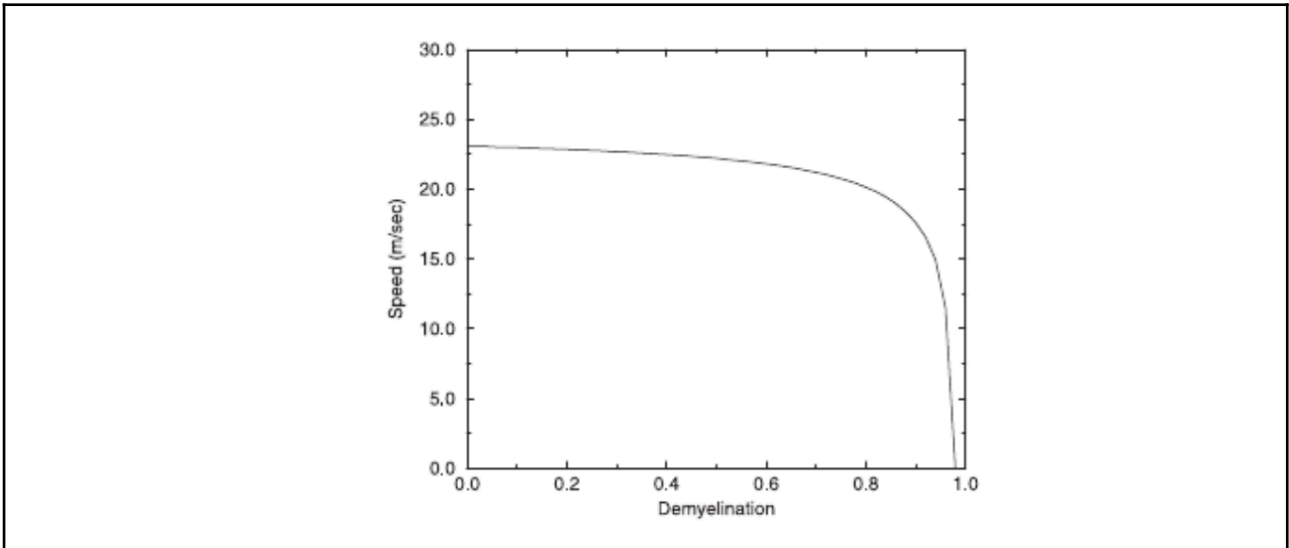


Fig. 7. Conduction velocity as a function of demyelination, from [12].

The base Hodgkin-Huxley model and internode model utilized constants from [16]. Code was written to modify each of the constant values by a step-size, for both the nodes and internodes, generating the figures in Appendix G; internode comparison tests were not included as it was observed that parameter changes did not change the waveform. Observationally, it was determined that the values from [16] and [28] yielded a waveform closest to the comparison waveform.

## V. DISCUSSION

In MS, the thinning of the myelin sheath is attributed to the remyelination process not fully regenerating the original thickness of the internodes in MS-afflicted tissue [17]. Saltatory conduction is a process where action potentials more quickly traverse the length of the axon via the movement of ions directly across internodes [18]. This is based on the insulating properties of the myelin sheath, allowing the transmission speed of the nerve impulses to be faster than in unmyelinated nodes [19]. Deterioration of the myelin sheath would likely undermine the process of saltatory conduction. As such, the expectation for Simulation 1 is a decrease in the conduction velocity. Research shows that there is a positive correlation in neurons between their conduction velocities and firing rates [20]. As such, an increase in the maximum firing rate given a constant injection current is expected.

Observing the results from Simulation 1, there is an exponentially increasing trend in conduction velocity and firing rate associated with increasing the myelin thickness, as shown in Fig. 1. A and B. This indicates that as the myelin thickness decreases, associated with the demyelination effect of MS, the conduction velocity also decreases. This ultimately supports the initial hypothesis that a reduction in myelin thickness of an internode leads to a decrease in conduction velocity and firing rate as it correlates to a slower transmission speed of nerve impulses. Varying the myelin thickness in Simulation 1 can be used to mimic the effectiveness of the remyelination process. Although the purpose of the remyelination process is to serve as a repair mechanism to recover demyelinated axons, the effectiveness of this process declines as MS progresses [21]. This was attributed to several reasons, primarily the exhaustion of the oligodendroglial progenitor cells, the cells used to regenerate myelin [21]. By observing the effect of varying myelin thickness on conduction velocity and firing rate, it can be seen that a decline in myelin regeneration (corresponding to regeneration of a smaller myelin thickness) will result in an overall lower conduction velocity and firing rate. This can ultimately be

used to quantify the relationship between reduction in myelin regeneration and its contribution to the severity of MS.

Similar trends are also observed in Simulation 2, which investigated the effects of increasing the number of demyelinated nodes on a neuron sequence. Fig. 2.A and B exhibit a decreasing trend in conduction velocity and firing rate as the number of demyelinated nodes increases. This is attributed to the insulation properties of the myelin sheaths that result in an increased conduction velocity [19].

The trend for conduction velocity is consistent across axons of different lengths. As can be seen from Fig. H.2, increasing the number of demyelinated nodes by a factor of 10 leads to roughly the same decrease in conduction velocity: going from 1 myelinated internode to 10 increases it by 1.024 m/s, going from 5 myelinated internodes to 50 increases in by 1.015 m/s. This suggests that a fixed proportion of internodes in an axon that becomes demyelinated (say 90% in this case) has a similar effect regardless of the length of the neuron. By successively demyelinating the internodes along an axon, the insulation previously supplied is removed and results in a lower conduction velocity. The same follows for the decreasing trend in firing rate as the number of demyelinated internodes is increased.

Although it is apparent in Fig. 1, 2, and 3 that the true velocity is shifted below the node velocity, it is evident that the trend of the true velocity mimics the behaviour of the node velocity. The apparent shift is attributed to the different velocity calculations, utilizing the axon length divided by the total time between the spike of the first and last node. Conversely, the estimated node velocity is calculated using the number of nodes, rather than the axon length.

Regarding the implications of these results on the progression of MS, it has been reported that a decrease in the conduction velocity of motor nerves is associated with decreased hand dexterity, a prominent symptom of MS [22, 23]. Hence, the findings reported in Simulation 1 and 2 could be employed to predict the decline in hand dexterity by monitoring the decreasing trend of conduction velocity as the myelin thickness decreases. The decline in firing rate resulting from the simulated demyelination of the internodes by way of varying the myelin thickness and ‘removal’ of the myelin at the internodes is also consistent with reported studies. While it has been reported that the electrical signals of the motor unit action potentials were normal in MS-afflicted brains, it was found that inconsistencies or variabilities in firing rate can be indicative of central or peripheral neurogenic weakness [24].

MS patients have been shown to exhibit a decline in their motor reaction time [26]. This may be related to the decrease in conduction velocity as a result of demyelination seen in simulations 1 and 2. One hypothesis would be that the weakening of saltatory conduction as a result of MS can lead to a slight increase in the amount of time for an impulse to process in the spinal cord (a site of MS) [1].

Given these findings, the results in Simulation 3 also follow a similar reasoning. Simulation 3 investigates how action potentials are slower when there are fewer internodes, as exhibited by the lower conduction velocity and firing rate. Results shown in Fig. 3 have an apparent increasing trend as the number of internodes increases. Given a fixed axon length, it is expected that decreasing the number of internodes, upon replacement by Nodes of Ranvier, results in decreased conduction velocity and firing rates [19]. This is due to the propagation of action potentials being comparatively slower in nodes than in internodes [19]. It is also important to note that while the trend in firing rate in Fig. 2.B and 3.B is linear, the firing rate in Fig. 1.B increases exponentially. This is mainly due to the scaling of the x-axis and the fact that as the myelin thickness continues to increase towards infinity, the insulating

properties of the myelin sheaths likely reach a maximum level of effectiveness. This could explain the observed plateauing of the firing rate around 0.0934 Hz.

Literature on the effects of nodal defects in CNS pathology reported that the lengthening of nodes may compromise the function of myelinated axons in MS, which in turn, may contribute to a decline in cognitive processing and motor output [25]. This effect of lengthening of nodes is effectively simulated in Simulation 3 when replacing internodes with nodes. Hence, modelling the rate at which the conduction velocity and firing rates as the number of nodes increases can be used to correlate and estimate a patient's decline in cognitive processing and motor output.

## VI. CONCLUSIONS AND RECOMMENDATIONS

The proposed neuron model is reflective of the behaviour of action potentials across an axon. Based on the findings of the three simulations, it was evident that the results supported the initial hypotheses. Firstly, Simulations 1 and 2 were successful at correlating the effects of gradual deterioration of myelin, as well as incomplete myelin restoration, onto conduction velocity and firing rate. Simulation 3 also established a positive correlation between myelination, by the abundance of internodes, and the speed of action potential transmission. The results of these findings were further confirmed during the verification tests performed on the model. The unit tests in section IV confirm the proper functionality of the model. The validation comparing the model results to experimental results on action potential behaviour at nodes and internodes supports that the model is consistent with the current literature. A limitation of this model, however, is the difficulty in accurately representing the lengths of nodes and internodes due to their variability. From literature, it was found that one internode has an average length of 1 mm while a node is around 2  $\mu\text{m}$ , given a constant axon length [11]. Thus, in order to accurately perform Simulation 3, a single node should be replaced with 500 nodes, making it a computationally expensive simulation as it would be executed 500 times. To simplify the simulation, a constant axon length was maintained.

Although the current model was validated by existing literature, further testing is necessary to enhance its accuracy. This includes conducting more comprehensive unit and regression testing to ensure that previously integrated functions continue to operate as expected following the implementation of the new changes mentioned above. Furthermore, although a positive correlation between saltatory conduction and firing rate can be observed in this model, and supported by literature, these results simply identify the type of trend, not an exact regression. Hence, implementing a function to quantitatively measure this correlation could yield interesting results and may have significant implications for the progression of MS symptoms such as reaction time, cognitive processing, and motor output [26].

## REFERENCES

- [1] R. Dutta and B. D. Trapp, “Mechanisms of neuronal dysfunction and degeneration in multiple sclerosis,” *Progress in Neurobiology*, vol. 93, no. 1, pp. 1–12, Jan. 2011.  
doi:10.1016/j.pneurobio.2010.09.005
- [2] Atlas of MS 3rd edition,  
<https://www.msif.org/wp-content/uploads/2020/10/Atlas-3rd-Edition-Epidemiology-report-EN-update-d-30-9-20.pdf> (accessed Apr. 8, 2024).
- [3] “About Multiple Sclerosis (MS),” *Pennmedicine.org*,  
<https://www.pennmedicine.org/for-patients-and-visitors/patient-information/conditions-treated-a-to-z/multiple-sclerosis-ms> (accessed Apr. 8, 2024).
- [4] C. L. Rice, T. L. Vollmer, and B. Bigland-Ritchie, “Neuromuscular responses of patients with multiple sclerosis,” *Muscle & Nerve*, vol. 15, no. 10, pp. 1123–1132, Oct. 1992.  
doi:10.1002/mus.880151011
- [5] S. L. Hauser and B. A. C. Cree, “Treatment of multiple sclerosis: A Review,” *The American Journal of Medicine*, vol. 133, no. 12, Dec. 2020. doi:10.1016/j.amjmed.2020.05.049
- [6] M. P. McGinley, C. H. Goldschmidt, and A. D. Rae-Grant, “Diagnosis and treatment of multiple sclerosis,” *JAMA*, vol. 325, no. 8, p. 765, Feb. 2021. doi:10.1001/jama.2020.26858
- [7] A. L. Hodgkin and A. F. Huxley, “A quantitative description of membrane current and its application to conduction and excitation in nerve,” *The Journal of Physiology*, vol. 117, no. 4, pp. 500–544, Aug. 1952. doi:10.1113/jphysiol.1952.sp004764
- [8] M. Zbili and D. Debanne, “Myelination Increases the Spatial Extent of Analog-Digital Modulation of Synaptic Transmission: A Modeling Study,” *Frontiers in Cellular Neuroscience*, vol. 14, Mar. 2020, doi: <https://doi.org/10.3389/fncel.2020.00040>. Available:  
<https://www.ncbi.nlm.nih.gov/pmc/articles/PMC7063086/>.
- [9] M. A. Latorre and K. Wårdell, “A comparison between single and double cable neuron models applicable to deep brain stimulation,” *Biomedical Physics & Engineering Express*, vol. 5, no. 2. IOP Publishing, p. 025026, Jan. 24, 2019. doi: 10.1088/2057-1976/aafdd9.
- [10] A. Salianni et al., “Axon and myelin morphology in animal and human spinal cord,” *Frontiers in Neuroanatomy*, vol. 11, Dec. 2017. doi:10.3389/fnana.2017.00129
- [11] D. C. Preston and B. E. Shapiro, “Anatomy and neurophysiology,” *Electromyography and Neuromuscular Disorders*, pp. 8–18, 2013. doi:10.1016/b978-1-4557-2672-1.00002-7

- [12] S. Reutskiy, E. Rossoni, and B. Tirozzi, "Conduction in bundles of demyelinated nerve fibers: Computer simulation," *Biological Cybernetics*, vol. 89, no. 6, pp. 439–448, Dec. 2003. doi:10.1007/s00422-003-0430-x
- [13] A. Rohatgi, WebPlotDigitizer, <https://apps.automeris.io/wpd/>.
- [14] S. Ibañez, N. Sengupta, J. I. Luebke, K. Wimmer, and C. M. Weaver, "Myelin dystrophy in the aging prefrontal cortex leads to impaired signal transmission and working memory decline: A Multiscale Computational Study, Sep. 2023. doi:10.1101/2023.08.30.555476
- [15] C. Solanes, J. L. Dura, J. De Andres, and J. Saiz, "What is the role of frequency on neural activation in tonic stimulation in SCS therapy? A computational study on sensory AB nerve fibers," *IEEE Access*, vol. 9, pp. 107446–107461, 2021. doi:10.1109/access.2021.3099986
- [16] T. Fortin, "Week 8 Tutorial Hodgkin-Huxley," LEARN, <https://learn.uwaterloo.ca/d2l/le/content/1004045/viewContent/5403878/View>.
- [17] I. D. Duncan, R. L. Marik, A. T. Broman, and M. Heidari, "Thin myelin sheaths as the hallmark of remyelination persist over time and preserve axon function," *Proceedings of the National Academy of Sciences*, vol. 114, no. 45, Oct. 2017, doi: <https://doi.org/10.1073/pnas.1714183114>.
- [18] C. C. H. Cohen et al., "Saltatory Conduction along Myelinated Axons Involves a Periaxonal Nanocircuit," *Cell*, vol. 180, no. 2. Elsevier BV, pp. 311-322.e15, Jan. 2020. doi: 10.1016/j.cell.2019.11.039.
- [19] E. N. Marieb, *Human Anatomy & Physiology*, 10th ed. London: Pearson Benjamin Cummings, 2012.
- [20] G. A. Jones, S. K. Norris, and Z. Henderson, "Conduction velocities and membrane properties of different classes of rat septohippocampal neurons recorded in vitro," *The Journal of Physiology*, vol. 517, no. 3. Wiley, pp. 867–877, Jun. 1999. doi: 10.1111/j.1469-7793.1999.0867s.x.
- [21] T. Goldschmidt, J. Antel, F. B. König, W. Brück, and T. Kuhlmann, "Remyelination capacity of the MS brain decreases with disease chronicity," *Neurology*, vol. 72, no. 22, pp. 1914–1921, Jun. 2009. doi:10.1212/wnl.0b013e3181a8260a
- [22] Y. Fukumoto, T. Wakisaka, K. Misawa, M. Hibi, and T. Suzuki, "Decreased nerve conduction velocity may be a predictor of fingertip dexterity and subjective complaints," *Experimental Brain Research*, vol. 241, no. 2, pp. 661–675, Jan. 2023. doi:10.1007/s00221-023-06556-2
- [23] J. L. Poole et al., "Dexterity, visual perception, and activities of daily living in persons with multiple sclerosis," *Occupational Therapy In Health Care*, vol. 24, no. 2, pp. 159–170, Mar. 2010. doi:10.3109/07380571003681202

- [24] L. J. Dorfman, J. E. Howard, and K. C. McGill, "Motor unit firing rates and firing rate variability in the detection of neuromuscular disorders," *Electroencephalography and Clinical Neurophysiology*, vol. 73, no. 3, pp. 215–224, Sep. 1989. doi:10.1016/0013-4694(89)90122-3
- [25] I. L. Arancibia-Carcamo and D. Attwell, "The node of ranvier in CNS pathology," *Acta Neuropathologica*, vol. 128, no. 2, pp. 161–175, Jun. 2014. doi:10.1007/s00401-014-1305-z
- [26] P. Elsass and I. Zeeberg, "Reaction time deficit in multiple sclerosis," *Acta Neurologica Scandinavica*, vol. 68, no. 4. Hindawi Limited, pp. 257–261, Oct. 1983. doi: 10.1111/j.1600-0404.1983.tb04835.x.
- [27] M. Zbili and D. Debanne, "Myelination Increases the Spatial Extent of Analog-Digital Modulation of Synaptic Transmission: A Modeling Study," *Frontiers in Cellular Neuroscience*, vol. 14, Mar. 2020, doi: <https://doi.org/10.3389/fncel.2020.00040>. Available: <https://www.ncbi.nlm.nih.gov/pmc/articles/PMC7063086/>.
- [28] J. W. Cooley and F. A. Dodge, "Digital Computer Solutions for Excitation and Propagation of the Nerve Impulse," *Biophysical Journal*, vol. 6, no. 5, pp. 583–599, Jan. 1966, doi: [https://doi.org/10.1016/s0006-3495\(66\)86679-1](https://doi.org/10.1016/s0006-3495(66)86679-1).
- [29] M. Zbili and D. Debanne, "Myelination Increases the Spatial Extent of Analog-Digital Modulation of Synaptic Transmission: A Modeling Study," *Frontiers in Cellular Neuroscience*, vol. 14, Mar. 2020, doi: <https://doi.org/10.3389/fncel.2020.00040>. Available: <https://www.ncbi.nlm.nih.gov/pmc/articles/PMC7063086/>.
- [30] M. A. Latorre and K. Wårdell, "A comparison between single and double cable neuron models applicable to deep brain stimulation," *Biomedical Physics & Engineering Express*, vol. 5, no. 2. IOP Publishing, p. 025026, Jan. 24, 2019. doi: 10.1088/2057-1976/aafdd9.

## Appendix A: Visualizations of Circuit Models

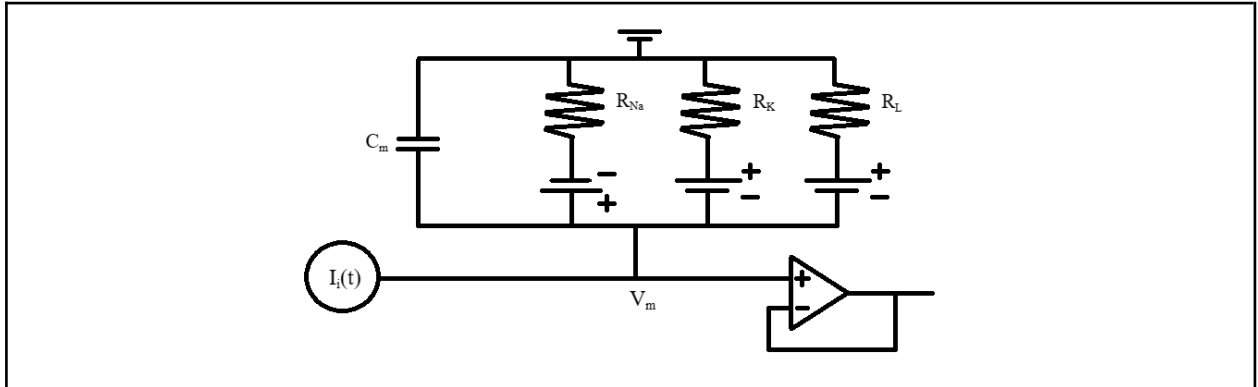


Fig. A.1. Circuit schematic of the Hodgkin-Huxley model with time-varying input  $I_i(t)$  and output  $V_m$ . Note that the grounded end represents the extracellular space matrix and the bottom-most end represents the intracellular medium; adapted from [7]; see Appendix C.3 for constants.

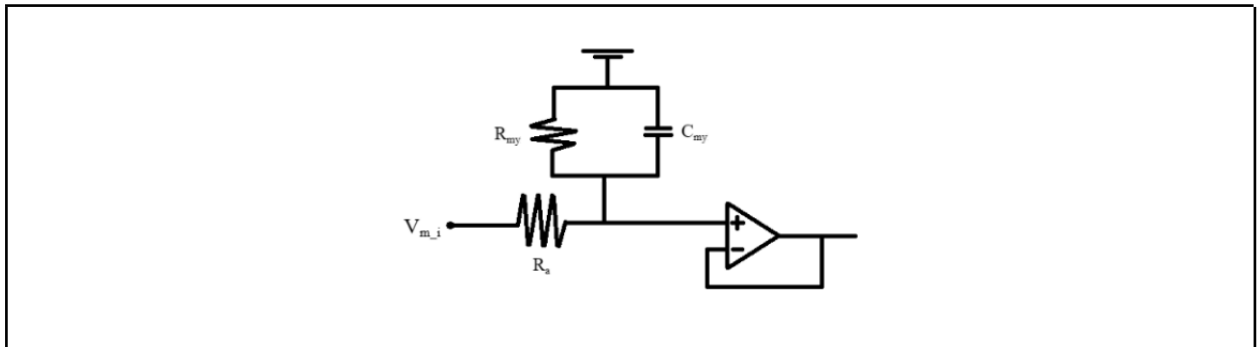


Fig. A.2. Circuit schematic of the single-cable internode model adapted from [9]; see Appendix C.3 for constants.

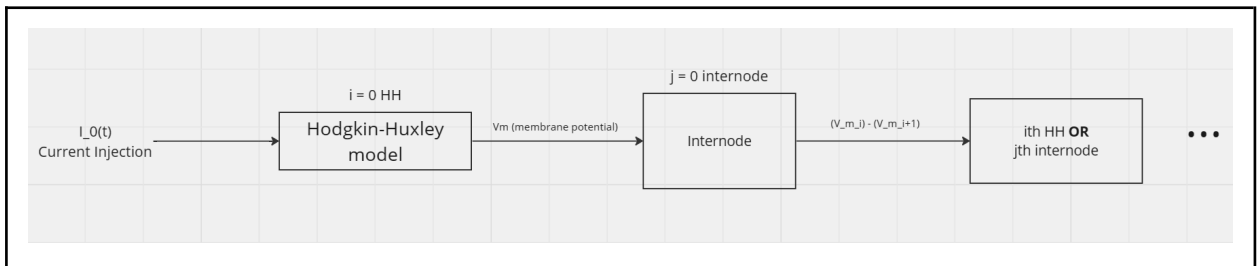


Fig. A.3. Block diagram of the model (sequence of nodes of internode will vary based on the simulation). The output of the entire system is a time-varying membrane voltage. The output of the entire system is a time-varying membrane voltage. See Appendix C.3 for constants.

## Appendix B: Derivation of State Equation for the Internode

Apply nodal analysis to the internode circuit in Fig. A.2:

$$\begin{aligned}\frac{V_m - V_0}{R_a} &= \frac{V_0}{R_L} + C_m(\dot{V}_0) \\ \frac{V_m}{R_a} - \frac{V_0}{R_a} - \frac{V_0}{R_L} &= C_m(\dot{V}_0) \\ \frac{V_m}{R_a} - V_0\left(\frac{1}{R_a} + \frac{1}{R_L}\right) &= C_m(\dot{V}_0)\end{aligned}$$

Thus,

$$\dot{V}_0 = -V_0\left(\frac{1}{C_{my}R_a} + \frac{1}{C_{my}R_{myi}}\right) + \frac{V_m}{C_{my}R_a}$$

Final state equation for the internode is also logged in Appendix C.4.2.

## Appendix C: Relevant Equations, Variable Functions and Definitions, Constant Values, and Complete State Equations

### C.1. Relevant Equations From [27]

$$g_{my} = g_L / (2n) \quad (C.1)$$

$$C_{my} = C_m / (2n) \quad (C.2)$$

### C.2. Variable Functions and Definitions

$$t_{my} = r_{ax}(0. \bar{6}) \quad (C.3)$$

Where  $t_{my}$  represents the thickness of the myelin sheath and  $r_{ax}$  represents the radius of the axon; this equation is adapted from [4].

$$n = \frac{t_{my}}{7.5 \text{ nm}} \quad (C.4)$$

Where  $n$  represents the number of myelin wraps and  $t_{my}$  represents the thickness of the myelin sheath; this equation is adapted from [4]

$$I_i(t) = \begin{cases} \text{current injection function, } i = 0 \\ \frac{V_i(t) - V_m(t)}{R_a} \end{cases} \quad (C.5)$$

Where  $I_i(t)$  is a time-varying current function, inputted into the  $i$ -th Hodgkin-Huxley segment (node) in a single axon model;  $V_i(t)$  represents the voltage outputted (and buffered) from the previous internode segment;  $V_m(t)$  represents the membrane potential/voltage for the  $i$ -th Hodgkin-Huxley segment;  $R_a$  represents the specific resistance of the axoplasm. The current injection function is an initial input to the entire axon; for the sake of simplicity, this may be a pulse function, but for more comprehensive simulations, data may be collected from literature to create an input function representing a current generated by a presynaptic neuron.



### C.3. Constant Values

- $r_{ax}$  = axonal radius (0.0238 cm) [28]
- $R_a$  = specific resistance of axoplasm (34.5 ohm cm) [28]
- $C_m$  = specific membrane capacitance (1 microF/cm<sup>2</sup>) [28]
- $g_{Na}$  = maximum sodium conductance (120 mmho/cm<sup>2</sup>) [28]
- $V_{Na}$  = sodium equilibrium potential (-115 mV) [16]
- $g_K$  = maximum potassium conductance (36 mmho/cm<sup>2</sup>) [28]
- $V_K$  = potassium equilibrium potential (12 mV) [16]
- $g_L$  = nonspecific leakage conductance (0.3 mmho/cm<sup>2</sup>) [28]
- $V_L$  = equilibrium potential of leakage current (-10.613 mV) [28]
- $R_{my}$  = resistance of the myelin sheath,  $1 / g_{my} = 2n / g_L = 2n / (0.3 \text{ mmho/cm}^2)$ , where n is number of myelin wraps [28, 29]
- $C_{my}$  = capacitance of the myelin sheath,  $C_m / (2n) = (1 \text{ microF/cm}^2) / (2n)$ , where n is number of myelin wraps [28, 29]

### C.4. State Equations

#### C.4.1 The Node (Hodgkin-Huxley)

From [7]:

$$I = C_m \dot{V}_m + g_K n^4 (V_m - V_K) + g_{Na} m^3 h (V_m - V_{Na}) + g_L (V_m - V_L), \text{ where}$$

$$\dot{n} = \alpha_n (1 - n) - \beta_n (n)$$

$$\dot{m} = \alpha_m (1 - m) - \beta_m (m)$$

$$\dot{h} = \alpha_h (1 - h) - \beta_h (h)$$

With state variables  $V_m$  (membrane potential),  $n$ ,  $m$ , and  $h$ , an input of  $I$ , and an output of  $V_m$ . Note that the equations for  $\alpha$  and  $\beta$  can be found in [17]. All other variables are constants; see Appendix C.3. Note also that a state-space form is not provided here as the model consists of non-linear differential equations.

#### C.4.2 The Internode

From [30]:

In state-space form, the internode state equation is:

$$\dot{V}_0 = -V_0 \left( \frac{1}{C_{my} R_a} + \frac{1}{C_{my} R_{myl}} \right) + \frac{V_m}{C_{my} R_a}$$

With state variables  $V_0$  and  $V_l$ , an input of  $V_m$  (the membrane potential of the previous section of the axon, represented by a Hodgkin-Huxley circuit), and an output of  $V_0$ . All other variables are constants; see Appendix C.2.

## Appendix D: MATLAB Function Implementations

### D.1. Conduction Velocity Function

```

1 function [node_over_time, length_over_time] = conduction_velocity(sequence,
2 voltage, time, axon_length)
...
19 if length(sequence) ~= rows
20     disp("ERROR IN conduction_velocity: STATE ARRAY MUST MATCH SEQUENCE");
21     node_over_time = -1;
22     length_over_time = -1;
23     return
24 end
25 % make sure that voltage array has same number of cols as there are
26 % time points in time array
27 if length(time) ~= cols
28     disp("ERROR IN conduction_velocity: STATE ARRAY MUST MATCH TIME ARRAY");
29     node_over_time = -1;
30     length_over_time = -1;
31     return
32 end
33 first_node = voltage(1, :);
34 last_node = voltage(length(sequence), :);
35
36 voltage_threshold = 0; % a spike will be considered a voltage > 0, this isn't
37 the best method
38
39 for i = 1:length(time)
40     % get first node peak
41     if first_node(i) > voltage_threshold
42         start_time = time(i);
43         break % peak found, don't accidentally grab time of next peak
44     end
45 end
46
47 for i = 1:length(time)
48     % get last node peak
49     if last_node(i) > voltage_threshold
50         end_time = time(i);
51         break % peak found, don't accidentally grab time of next peak
52     end
53 end
54 node_over_time = length(sequence) / (end_time - start_time);
55
56 % optional argument: length of axon in mm
57 if nargin == 4
58     length_over_time = axon_length / (end_time - start_time);
59 else
60     % if no length is passed, then set to 0

```

```

61         length_over_time = 0;
62     end
63 end

```

## D.2. Firing Rate Function

```

1  function [firing_rate, pks, locs] = get_firing_rate(output, time)
2
3      [rows, cols] = size(output);
4
5      % make sure that voltage array has same number of cols as there are
6      % time points in time array
7      if length(time) ~= cols
8          disp("ERROR IN conduction_velocity: STATE ARRAY MUST MATCH TIME ARRAY");
9          firing_rate = -1;
10         return
11     end
12
13     % extract voltage sequence at last node from output matrix
14     voltage_at_last_node = output(rows, :);
15
16     % find AP spikes
17     [AP_spikes, AP_times] = findpeaks(voltage_at_last_node, time, MinPeakHeight=10);
18     firing_rate = length(AP_spikes) / (AP_times(end) - AP_times(1));
19
20     pks = AP_spikes;
21     locs = AP_times;
22 end

```

## Appendix E: MATLAB Simulation Implementations

### E.1. Simulation 1

```

1  %% simulation 1: vary myelination of internodes
2  function sim1_vary_myelin(number_of_internodes, starting_myelin, end_myelin,
3  step_size)
4      % use the neuron class
5      % plot conduction velocity vs myelin thickness
6      % plot firing rate vs myelin thickness
7      % constant amount of internodes
8      % start at x myelin thickness and decrement by fixed amount until reaching zero
9      % At each myelin thickness we need to make note of firing rate, and
10     % output velocity
11     if nargin < 4
12         step_size = 7.5;
13     end
14     % Constants
15     internode_length = 1; % in mm;
16     node_length = 2 / 1000; % in mm;
17     % Initialize Output Arrays
18     conduction_node_velocities = [];
19     conduction_true_velocities = [];
20     firing_rates = [];
21     % Set up the sequence array based on the number_of_internodes
22     sequence_array = zeros(1, 2*number_of_internodes + 1);
23     sequence_array(2:2:end-1) = 1;
24     % Calculate axon length
25     number_of_nodes = length(sequence_array) - number_of_internodes;
26     axon_length = number_of_internodes * internode_length + number_of_nodes *
27     node_length;
28     % Generate the array of myelin thicknesses
29     myelin_values = starting_myelin:step_size:end_myelin;
30     % Simulate for each thickness and add to the velocity and firing rates
31     for i = 1:length(myelin_values)
32         % Access and print the current myelin value
33         myelin_value = myelin_values(i);
34         [output, time] = simulate_internode_node_sequence(sequence_array,
35 myelin_value);
36         [conduction_velocity_node, conduction_velocity_true] =
37 conduction_velocity(sequence_array, output, time, axon_length);
38         conduction_node_velocities = [conduction_node_velocities,
39 conduction_velocity_node];
40         conduction_true_velocities = [conduction_true_velocities,
41 conduction_velocity_true];
42         firing_rates = [firing_rates, get_firing_rate(output,time)];
43     end
44
45     % PLOTTING CODE HERE
46     figure()
47     FontSize = 12;
48     LineWidth = 1.5;

```

```

49 % Your plotting code should be here
50 plot(myelin_values, conduction_node_velocities, 'LineWidth', LineWidth)
51 hold on;
52 plot(myelin_values, conduction_true_velocities, 'LineWidth', LineWidth)
53 hold off;
54
55 legend('Node Velocity (node/ms)', 'True Velocity (m/s)') % note the order here
56 xlabel('Myelin Thickness (nm)')
57 ylabel('Velocity')
58 set(gca, 'FontSize', FontSize)
59 figure()
60 plot(myelin_values, firing_rates, 'LineWidth', LineWidth)
61 xlabel('Myelin Thickness (nm)')
62 ylabel('Firing Rate (Hz)')
63 set(gca, 'FontSize', FontSize)
64 figure()
65 plot(conduction_true_velocities, firing_rates, 'LineWidth', LineWidth)
66 xlabel('True Conduction Velocity (m/s)')
67 ylabel('Firing Rate (Hz)')
68 set(gca, 'FontSize', FontSize)
69 disp(myelin_values);
70 end

```

## E.2. Simulation 2

```

1 %% simulation 2: remove myelin from internodes
2 function sim2_demyelinated_internode(number_of_internodes)
3 % use the neuron class
4 % plot conduction velocity vs # of demyelinated internodes
5 % plot firing rate vs # of demyelinated internodes
6 % neuron length is constant
7 % in this experiment myelin will be "removed" from one internode at a
8 % time. the number of nodes and internodes are kept constant.
9 % myelin wraps (n) will be set to 0.5 for all (which is approx 4nm of myelin)
10 % Constants
11 internode_length = 1; % in mm;
12 node_length = 2 / 1000; % in mm;
13 myelin_thickness = 250; % in nm
14 % Initialize Output Arrays
15 conduction_node_velocities = [];
16 conduction_true_velocities = [];
17 firing_rates = [];
18 demyelinated_node_array = [];
19 % Set up the sequence array based on the number_of_internodes
20 sequence_array = zeros(1, 2*number_of_internodes + 1);
21 sequence_array(2:2:end-1) = 1;
22 % Calculate axon length
23 number_of_nodes = length(sequence_array) - number_of_internodes;
24 axon_length = number_of_internodes * internode_length + number_of_nodes *
25 node_length;
26 % Demyelinate and add to the arrays

```

```

27     for i = 0:number_of_internodes
28         [output, time] = simulate_internode_node_sequence(sequence_array,
29 myelin_thickness, i);
30         [conduction_velocity_node, conduction_velocity_true] =
31 conduction_velocity(sequence_array, output, time, axon_length);
32         conduction_node_velocities = [conduction_node_velocities,
33 conduction_velocity_node];
34         conduction_true_velocities = [conduction_true_velocities,
35 conduction_velocity_true];
36         firing_rates = [firing_rates, get_firing_rate(output,time)];
37         demyelinated_node_array = [demyelinated_node_array, i];
38     end
39     % PLOTTING CODE HERE
40     figure()
41     FontSize = 12;
42     LineWidth = 1.5;
43     % Your plotting code should be here
44     plot(demyelinated_node_array, conduction_node_velocities, 'LineWidth',
45 LineWidth)
46     hold on;
47     plot(demyelinated_node_array, conduction_true_velocities, 'LineWidth',
48 LineWidth)
49     hold off;
50
51     legend('Node Velocity (node/ms)', 'True Velocity (m/s)') % note the order here
52     xlabel('Demyelinated Nodes (nm)')
53     ylabel('Velocity')
54     set(gca, 'FontSize', FontSize)
55     figure()
56     plot(demyelinated_node_array, firing_rates, 'LineWidth', LineWidth)
57     xlabel('Demyelinated Nodes (nm)')
58     ylabel('Firing Rate (Hz)')
59     set(gca, 'FontSize', FontSize)
60     figure()
61     plot(conduction_true_velocities, firing_rates, 'LineWidth', LineWidth)
62     xlabel('True Conduction Velocity (m/s)')
63     ylabel('Firing Rate (Hz)')
64     set(gca, 'FontSize', FontSize)
65 end

```

### E.3. Simulation 3

```

1  %% simulation 3: replace internodes with HH nodes
2
3  function sim3_internode_to_node(number_of_internodes)
4      % use the neuron class
5      % plot conduction velocity vs # of internodes
6      % plot firing rate vs # of internodes
7      % neuron length is constant
8
9      % in this experiment internodes will be replaced with HH nodes one at a

```

```

10 % time. the total number of segments is kept constant. the amount of
11 % myelin in remaining internodes should be kept constant, with some
12 % level of random noise.
13
14 % Set Constants
15 internode_length = 1; % in mm;
16 node_length = 2 / 1000; % in mm;
17 myelin_thickness = 500; % in nm
18
19 % Initialize number_of_internodes array
20 number_of_internodes_plot = [];
21 conduction_node_velocities = [];
22 conduction_true_velocities = [];
23 firing_rates = [];
24 for i = number_of_internodes:-1:0
25     number_of_internodes_plot = [number_of_internodes_plot, i];
26 end
27
28 % Initialize the array with alternating 1s and 0s, starting and ending with 0
29 initial_array = zeros(1, 2*number_of_internodes + 1);
30 initial_array(2:2:end-1) = 1;
31 flipped_array = initial_array;
32
33 % Set axonal length
34 number_of_nodes = length(initial_array) - number_of_internodes;
35 axonal_length = number_of_internodes * internode_length + number_of_nodes *
36 node_length;
37
38 %Initial Array Code
39 [output, time] = simulate_internode_node_sequence(initial_array,
40 myelin_thickness);
41 % Get the conduction velocity and firing rate
42 [conduction_velocity_node, conduction_velocity_true] =
43 get_conduction_velocity(number_of_internodes, initial_array, output, time);
44 conduction_node_velocities = [conduction_node_velocities,
45 conduction_velocity_node];
46 conduction_true_velocities = [conduction_true_velocities,
47 conduction_velocity_true];
48 firing_rates = [firing_rates, get_firing_rate(output,time)];
49
50 % Flip each 1 to a 0 sequentially
51 for i = 2:2:length(flipped_array)-1
52     flipped_array(i) = 0;
53     number_of_internodes = number_of_internodes - 1;
54     % Work With AdjustedArray
55     [output, time] = simulate_internode_node_sequence(flipped_array,
56 myelin_thickness);
57     % Get the conduction velocity and the firing rate
58     [conduction_velocity_node, conduction_velocity_true] =
59 get_conduction_velocity(number_of_internodes, initial_array, output, time);
60 conduction_node_velocities = [conduction_node_velocities,

```

```

61 conduction_velocity_node];
62     conduction_true_velocities = [conduction_true_velocities,
63 conduction_velocity_true];
64     firing_rates = [firing_rates, get_firing_rate(output,time)];
65 end
66     function [node_velocity, true_velocity] = get_conduction_velocity(internodes,
67 sequence_array, neuron_output, neuron_time)
68         % dynamic length below
69         dynamic_length = internodes * internode_length + number_of_nodes *
70 node_length;
71         % Use sequence array for dynamic calculation
72         [node_velocity, true_velocity] = conduction_velocity(initial_array,
73 neuron_output, neuron_time, axonal_length);
74     end
75     % PLOTTING CODE HERE
76     figure()
77     FontSize = 12;
78     % Your plotting code should be here
79     plot(number_of_internodes_plot, conduction_node_velocities)
80     hold on;
81     plot(number_of_internodes_plot, conduction_true_velocities)
82     hold off;
83
84     legend('Node Velocity', 'True Velocity') % note the order here
85     xlabel('Number of Internodes')
86     ylabel('Velocity')
87     set(gca, 'FontSize', FontSize)
88     figure()
89     FontSize = 12;
90     plot(number_of_internodes_plot, firing_rates)
91     xlabel('Number of Internodes')
92     ylabel('Firing Rate')
93 end

```

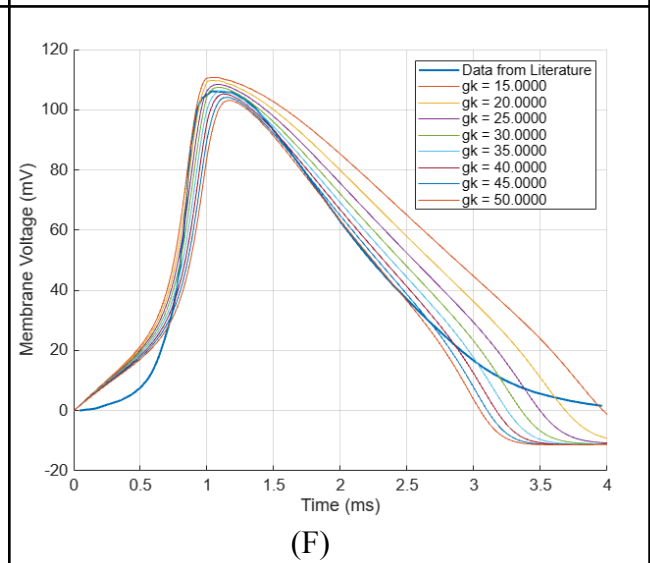
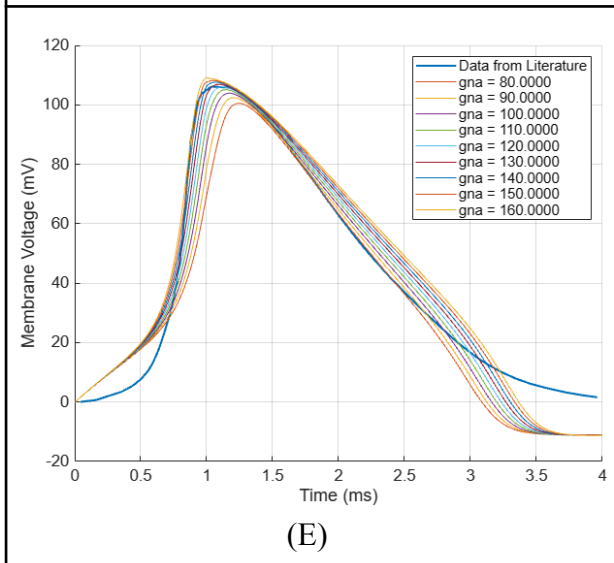
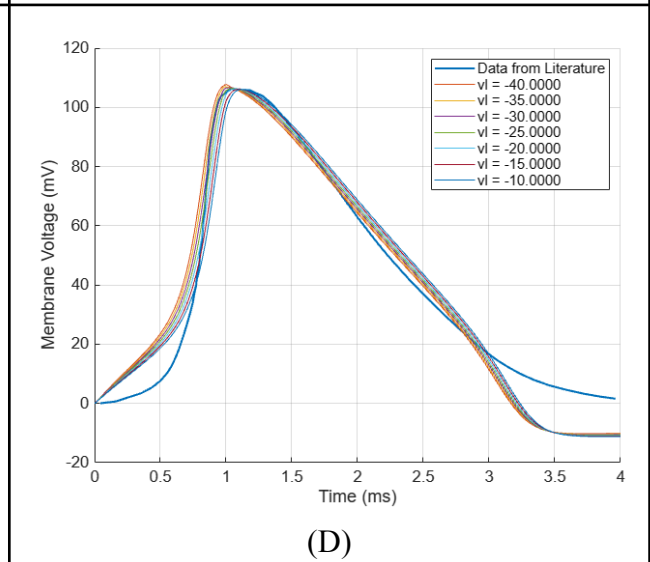
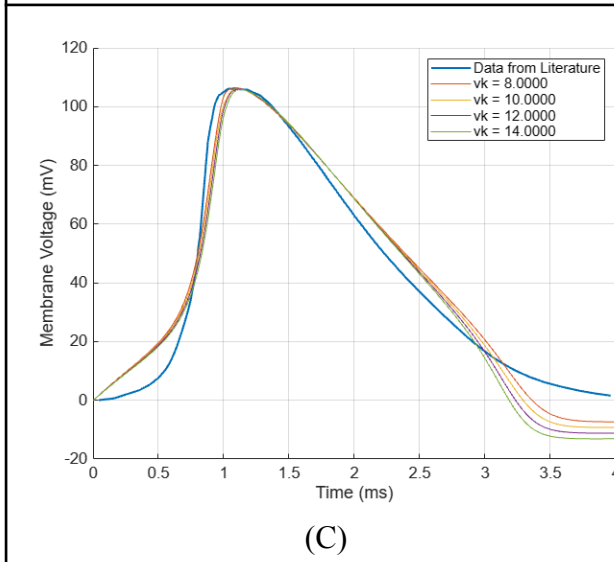
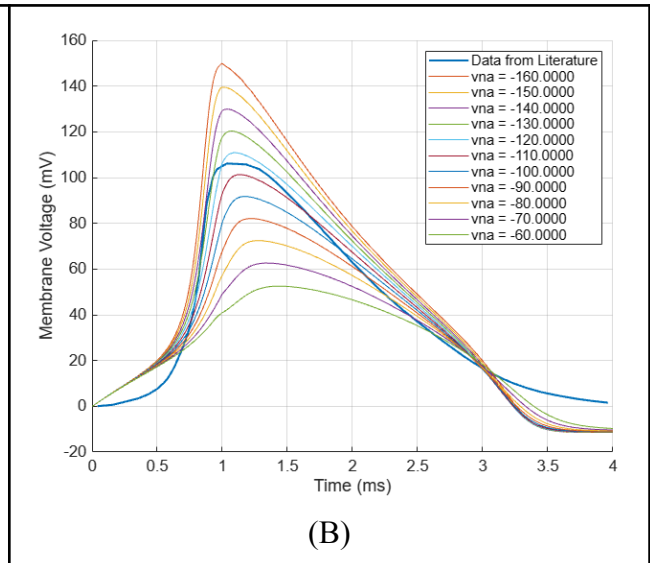
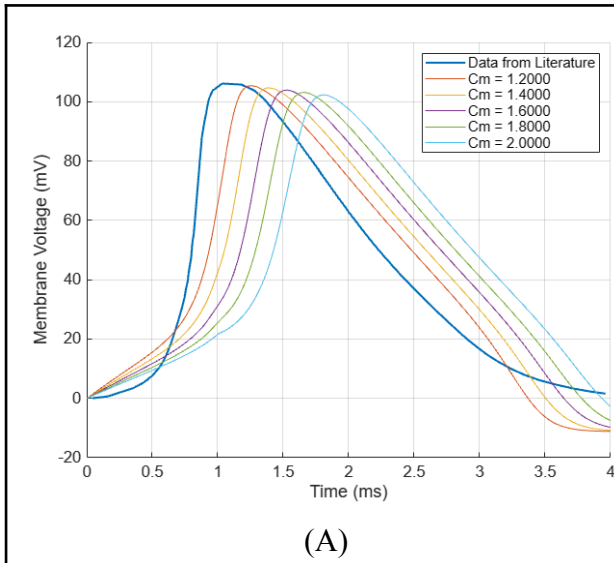


## Appendix F: Verification Unit Tests

TABLE F.1. VERIFICATION ACTIVITIES SUMMARY AND RESULTS

Unit Test ID (if applicable).	Activity Description.	Test Result.
Code Review.		
-	Review the internode state equation; compared to Appendix C.4.	PASS.
-	Review the HH state equations; compared to Appendix C.4.	PASS.
-	Review the input function used for HH nodes after the starting node; compared to Equation (C.5).	PASS.
Unit Tests.		
testConductionVelocity() ( )	Test conduction_velocity() using the following input arguments: <ul style="list-style-type: none"> <li>• sequence = [0 1 0]</li> <li>• voltage = [1 -1 -1; -1 -1 -1; -1 -1 1]</li> <li>• time = [0 1 2]</li> <li>• axon_length = 1</li> </ul> Confirm that nodal velocity is 1.5 and true velocity is 0.5.	PASS.
testFiringRate() ( )	Test firing_rate() by passing it a sawtooth wave and the corresponding time array. Confirm that firing rate is equal to the wave's frequency (Hz)	PASS.
testConstructorWithStartingNodeTrue()  testConstructorWithStartingNodeFalse() ( )	Confirm that the HodgkinHuxley constructor assigns values correctly.	PASS.
testConstructorInternode() ( )	Confirm that the Internode constructor assigns values correctly.	PASS.
testAddSegment() ( )	Confirm that Neuron.add_segment stores parameters correctly.	PASS.

## Appendix G: Optimization Figures



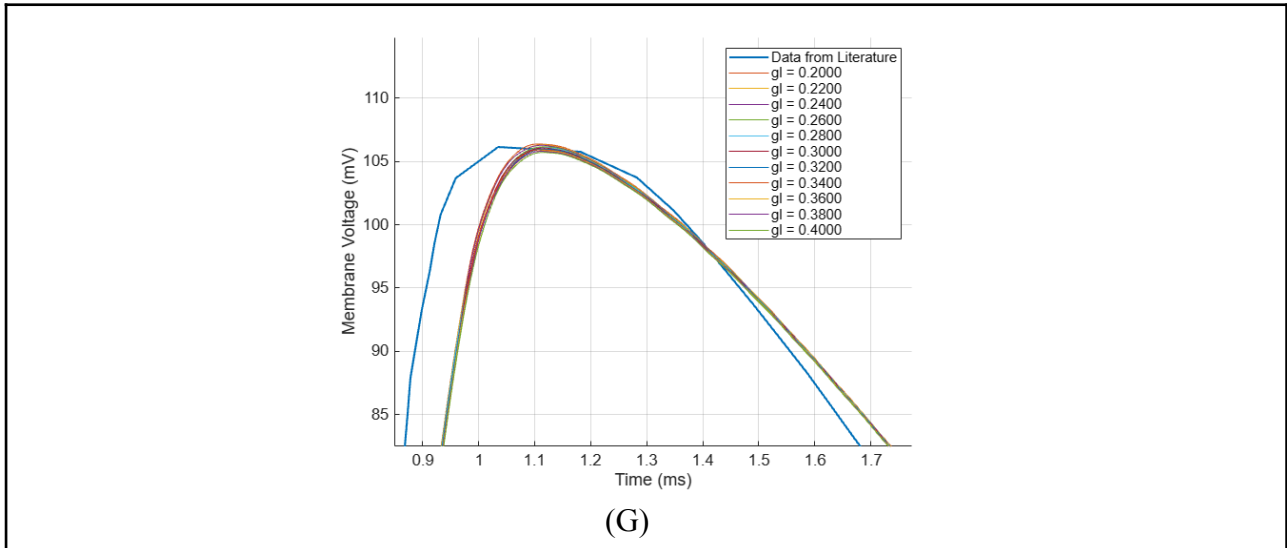


Fig. G.1. Optimization of H-H node constant parameters compared to data from [12].

## Appendix H: Additional Findings

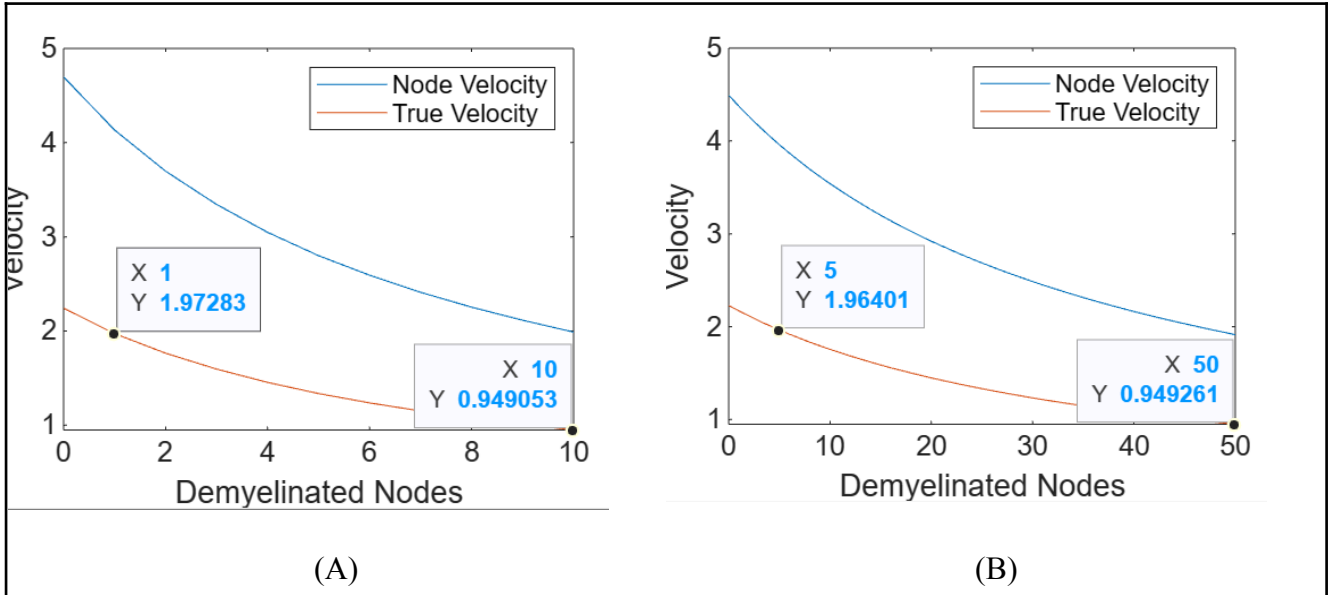


Fig. H.1. (A)-(B) Comparison between the effect of demyelination on conduction velocity of axons of different numbers of internodes (and thus different lengths)

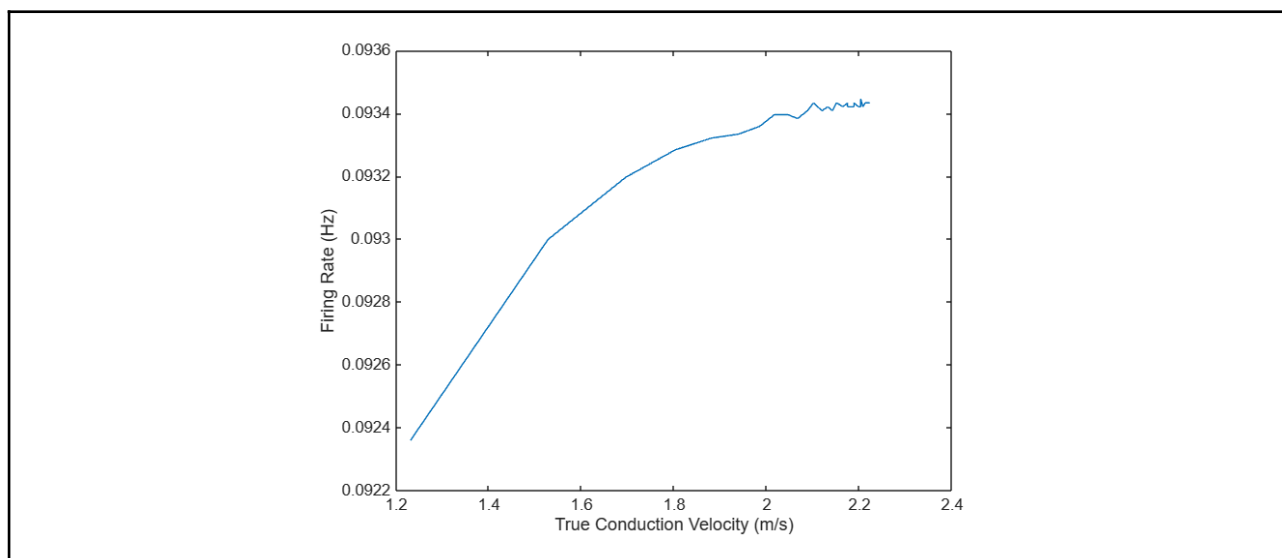


Fig. H.2. Relationship between firing rate and conduction velocity (acquired from Simulation 1).